

Experimental Performance Evaluation of Solar Parabolic-Trough Collector Using Solar Topocentric Coordinates Of Bauchi, Nigeria

I. S. Sintali

Department of Mechanical Engineering, Faculty of Engineering and Engineering Technology, Abubakar Tafawa Balewa University, Bauchi, Nigeria

ABSTRACT: This paper presents the experimental performance evaluation of a Solar Parabolic-Trough Collector (SPTC) Model TE 38 using solar topocentric coordinates of Bauchi. The results show that the effects of using solar coordinates influence the performance of the collector to certain extent. The hourly thermal performance of the collector increased with time as the incidence and tracking angle increases. The maximum hourly temperatures of the glass-cover, absorber-tube and working fluid attained are 58.3°C, 148.4°C and 132.7°C respectively. It was also observed that the hourly thermal efficiencies of the collector computed increased with increase in both incidence and tracking angles with time and the maximum attained was 85.9%. The hourly absorber-tube temperatures attained experimentally are capable of boiling water and other low boiling point coolant for steam generation and thus for electricity generation and other solar water applications. The system can be scale up for energy generation and integration into the national energy mix of Nigeria.

Keywords: Parabolic-trough, thermal performance, topocentric angles, thermal efficiency, glass-cover, absorber-tube and working fluid.

I. INTRODUCTION

1.1 Background of the Study

Man has needed and used energy at an increasing rate for his sustenance and wellbeing ever since he came on earth million years ago. Energy is an essential input to all aspects of modern age and indeed, the life wire of industrial and agricultural production, the fuel for transportation as well as for the generation of electricity in conventional thermal power plants.

Inadequate supply of energy restricts socio-economic activities, limits economic growth and adversely affects the quality of life. This implies that the level of energy utilization in an economy, coupled with the efficiency of conversion of energy resources to useful energy, is direct indicative of the level of development of the economy. Thus, Nigeria's future energy requirements will continue to grow with increase in living standards, industrialization and a host of other socio-economic factors. Consequently, apart from being finite, the conventional energy resources such as crude oil, natural gas and other fossil fuels alone will not meet the challenges of an increasing demand for energy at affordable cost and in a flexible manner. Thus, finding ways to expand energy services while simultaneously addressing the environmental impacts associated with energy use represents a critical challenge to humanity.

In line with Rio de Janeiro United Nations Conference on Environment and Development (UNCED) [1], the Federal Government of Nigeria approved energy policy for the country in 2003, in which provisions were made for the coordinated development, utilization and management of all energy resources. The document admits that grids extension through conventional (petroleum products, gas, coal electricity) alone will not meet universal rural electrification coverage cost-effectively within a reasonable timeframe and thus makes adequate allowance for rural energy supply with non-conventional and renewable (solar, wind, small-scale hydro, biomass, fuel wood etc.) alternatives. Emphases were particularly placed on solar and biomass energy resources and integrating it into the national energy mix. These are yet to be fully integrated into the system except for some piloting effort by Energy Commission of Nigeria (ECN) in some selected locations in the country.

In as much as there is potentially large amount of energy available from the sun, systems require to capture, concentrate and convert the thermal energy must perform efficiently at a cost competitive with other forms of energy. Thus, for efficient collection of solar radiation using solar parabolic-trough collector (SPTC),

model equations for the predictions of solar position in Bauchi were developed and simulated by Sintali *et al*[2]. The experimental performance evaluation of the SPTC (Model TE 38) carried out was aimed at validating the developed energy equations.

The experiment conducted involves the use of SPTC (Model TE38) shown in Plate I and it was obtained from Thermodynamics laboratory of the Department of Mechanical/Production Engineering, Abubakar Tafawa Balewa University (ATBU), Bauchi. The rig comprising the parabolic-trough collector, receiver assembly and thermocouple probes to measure temperatures of the glass cover, absorber-tube and the fluid was mounted at ZERI, a research center in ATBU, Bauchi. Other meteorological measuring instruments used in taking the readings of global and diffuse radiations; wind speed and daily ambient temperature of Bauchi are all discussed.



Plate I: Parabolic-Trough Concentrator (Model TE38)

II. MATERIALS

2.1 Solar Parabolic-Trough Collector Model TE38

The SPTC Model TE38 consists of a reflecting surface made by bending highly polished stainless steel reflector and fixed on a parabolic contour. The parabolic contour is supported by steel framework and mounted on a reflector support structure. Tilting mechanism permits adjustment of declination, in order to track the sun, thus, maintains the focusing of the solar radiation on the receiver. The receiver assembly comprises of the absorber-tube covered with a glass-cover tube to reduce heat losses, is placed along the focal line of the receiver as shown in Plate I. The SPTC has the following data[3]:

- | | | | |
|-------------|----------------------------|---|--------------------|
| i. | Inclination and azimuth | - | Adjustable |
| ii. | Parabolic reflector | - | Stainless Steel |
| iii. | Aperture width(w) | - | 800mm (0.8m) |
| iv. | Collector length (L) | - | 300mm(0.3m) |
| v. | Focal length(f) | - | 487mm (0.487) |
| vi. | Aperture area (A_a) | - | 0.24m ² |
| vii. | Rim angle (ψ_{rim}) | - | 45° |

2.2 Absorber-tube Materials/Design

The energy collector system (the receiver assembly comprising of the absorber-tube and the enveloping glass-cover) was constructed using Pyrex glass and copper tube. The absorber-tube material has an external diameter of 13mm and a thickness of 2mm and total length of 450mm. The high thermal conductivity of copper coupled with the small size of the tube allow for low thermal resistance. A thermocouple was embedded on the absorber-tube surface. This was used to measure the temperatures of the absorber-tube during experimentation. The copper tube is coated with emulsion black paint that has low emittance thermal property, increases the absorptance of the incident solar irradiance and reduces simultaneously the reflectance. The Absorber-tube is shown in Figure 1.

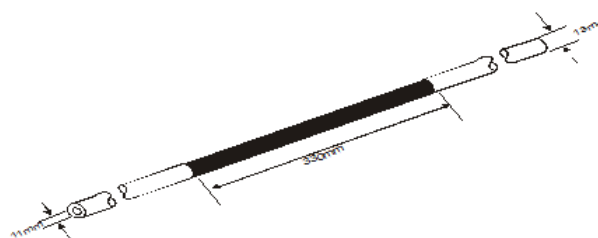


Fig.1: Schematic representation of the Absorber-tube

2.3 Glass Cover Materials/Design

The absorber-tube is covered concentrically with an enveloping glass-cover made of Pyrex glass-tube of 385mm length. According to Harrison [4] borosilicate glass (Pyrex) is ideally suited material for the absorber-tube cover, because it withstands high temperature and is a tough glass material that can withstand heat and solar radiation. The enveloping glass-cover material as shown in Figure 2 has an external diameter of 41mm and internal diameter 38mm. The space between the glass-cover tube and the absorber-tube was hermetically closed and evacuated. The internal pressure was assumed less than the atmospheric pressure after evacuation. The usefulness of the enveloping glass-tube cover is significant, since it eliminates the convective heat loss and reduces the heat losses due to radiation, because the produced heat from the absorber-tube is trapped.

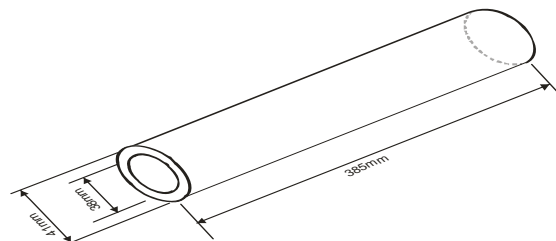


Fig.2: Schematic representation of the enveloping glass-cover

2.4 Receiver Assembly

The receiver assembly, comprises of the absorber tube located at the focal axis through which the liquid to be heated flows and the concentric-transparent glass-cover to reduce the convective heat transfer. The opening gap between the glass-cover tube and the absorber-tube at the two ends was closed with “*Gmelina arborea*” wood that was covered with rubber bonding adhesives to make it leak-proof. The annular gap was evacuated using a vacuum pump VP1 PUMP SERIES obtained from Chemistry Laboratory of the ATBU, Bauchi. The vacuum pump is shown in Plate II. The internal pressure was assumed less than the atmospheric pressure after evacuation. The receiver assembly is shown in Plate III.



Plate II: Pictorial view of the Vacuum Pump (VP1 PUMP)

The vacuum pump does not have a meter. The Operating Manual specified that evacuation should be carried out by connecting a suitable tube to the inlet connector point i.e. the suction point to the extractable object, (the receiver assembly) and presses the green illuminated switch to the “on” position. Observing the pressure surge then continuously monitors the exhaust point. The complete evacuation is assumed successful when no air comes out from the exhaust point.



Plate III: The receiver assembly

2.5 Setting of the Test Rig

In setting of the test rig digital compass was used in obtaining the correct east-west and north-south directions and with the aid of plum the turn-table that carries the collector assembly was balanced. The top of the turn-table was graduated into angles (-180° to $+180^{\circ}$) to obtain the azimuth angles. The collector was then mounted on the turn-table with one of its center side being marked as a reference point against the graduated angles on the turn-table and this was used in getting the hourly azimuth angles. The receiver assembly comprises of the absorber-tube covered with a glass-cover to reduce heat losses, was placed along the focal line of the collector as shown in Plate I. Thus, by turning the collector on the turn-table and adjusting the tracking mechanism, the focusing of solar radiations onto the receiver were achieved. The angle on the turn table that coincides with the reference on the collector gives the azimuth angle and the monthly average results obtained are being recorded.

The experimental solar altitude angles (α) being a complement of zenith angles were obtained by subtracting the zenith angle from 90° (i.e. $90^{\circ} - \theta_z$). The experiment was carried out at the premises of ZERI CENTER of the ATBU, Bauchi.

2.6 Measuring Instruments

2.6.1 Wind Speed and Ambient Temperature

The hourly wind speed and ambient temperature are measured with the aid of “Automatic Weather Station, Vantage Pro2” meteorological instrument shown in Plate IV and Plate V.



Plate IV: Pictorial view of the wind and atmospheric temperature sensor

Plate VI shows the pictorial view of the wind and ambient temperature sensor of the “Automatic Weather Station” used in taking the readings of wind speed and ambient temperature. This part of the instrument was mounted on top of a mass. The base station, from where readings are taken, was placed on a table in an office and readings are taken hourly as shown in Plate V.



Plate V: Pictorial view of the base station

2.6.2. Solarimeter

The Solarimeter used for the measurement of global radiation consists of a series of a thermocouple junctions connected to a series of silver segments, coloured alternatively black and white, and covered by a hemispherical frosted glass dome. The calibrated apparatus gives an output proportional to the total incident radiation for general use.



Plate VI: Pictorial view of Plint Solarimeter

The Solarimeter was mounted horizontally in a position in which it can “see” the whole hemisphere of the sky as shown in plate VI. Its reading then gives a good indication of the total energy, direct plus diffuse, arriving at the collector surface.

2.6.3. Pyranometer

The diffuse component of the global radiation was measured by Pyranometer CM11 as shown in Plate VII below. The Pyranometer used consists of a shadow band used to block beam radiation.



Plate VII: Pictorial view of Pyranometer CM .11

2.6.4 Digital Thermometer

A two way Kane-May (KM340) digital thermometer was used in taking the readings of glass-cover, absorber-tube and fluid temperatures in an interval of an hour. The digital thermometer as shown in Plate VIII is capable of taking temperature measurement up to a maximum of 1000°C. It uses thermocouples; one of the couple was inserted into the absorber-tube to measure the temperature of the fluid; another couple was tied to the absorber tube to measure the temperature of the tube and the tip of another couple was placed on the glass-cover to measure the temperature of the glass-cover tube.



Plate VIII: Kane-May (KM340) Digital Thermometer

III. METHODS

3.1 Meteorological Data

The hourly global and diffuse radiations were obtained using Solarimeter and Pyranometer respectively while the hourly wind speed and surface temperatures (ambient) were obtained using “Automatic Weather Station *Vantage PRO2*”. The values obtained are used in computing the hourly thermal efficiency of the solar parabolic-trough concentrating collector (Model TE .38).

3.2 Computation of Solar Coordinates

The energy equations developed by Sintali *et al* [2] were adapted in computing the collector thermal performances and solar coordinates in Bauchi. The heliocentric, geocentric and topocentric coordinates were all considered in determining the solar coordinates. The latitude and longitude of Bauchi considered are 9.81° E and 10.33° N respectively [5].

3.2.1 Topocentric Azimuth angle (A)

The local topocentric azimuth angles were obtained using the graduated angles on the turn table against a reference point on the collector. One center side of the collector was marked and served as a reference point against the graduated angles on the turn table. By turning the collector on the turn-table and adjusting the hand wheel, the solar beam from the reflecting surface of the collector would be focused onto the receiver. The angle on the turn table that coincides with the reference on the collector gives the azimuth angle as shown in plate IX.



Plate IX: Azimuth Angle Scale on the Turn-Table

3.2.2 Topocentric Zenith angle (θ_z)

The solar zenith angle θ_z is the angle between a solar ray and local vertical direction as illustrated in Plate X.



Plate X: Solar Zenith Angles Scale

3.2.3 Topocentric Altitude angle (α)

The solar altitude angle α at a point on the earth is the angle between the line passing through the point and the sun and the line passing through the point tangent to the earth and passing below the sun. α is a complement of the zenith angle θ_z . The angles were obtained by subtracting θ_z from 90° (i.e. $90^\circ - \theta_z$).

3.2.4 Solar incidence angle θ_i

In the design of solar energy systems, it is most important to be able to predict the angle between the sun's rays and a vector normal to the aperture or surface of the collector. This angle is called the angle of incidence θ_i ; the maximum amount of solar radiation reaching the surface (or geometric aperture) is reduced by cosine of this angle. The other angle of importance is the tracking angle ρ_t . For practical application when the tracking axis is oriented in the north-south direction, then incidence angle θ_i and the tracking angle ρ_t are given by equation 1 and 2 respectively [6].

$$\cos \theta_i = \sqrt{1 - \cos^2 \alpha \cos^2 A} \quad \text{Eqn. 1}$$

$$\tan \rho_t = \frac{\sin A}{\tan \alpha} \quad \text{Eqn. 2}$$

3.3 The Thermal Efficiency of the Parabolic-Trough Collector (η_{th})

The thermal efficiency of the Parabolic-trough Collector is given by;

$$\eta_{th} = 1 - \frac{Q_{losses}}{Q_{input}} \quad \text{Eqn. 3}$$

Where Q_{losses} is the total heat losses and Q_{input} is the total heat supplied to the receiver.

The hourly heat supplied to the receiver (Q_{input}) can be computed as follows:

$$Q_{input} = [(I_{beam} * R_b) + I_{diff}] [WL] \quad \text{Eqn. 4}$$

Where $I_{beam} * R_b$ is the beam radiation on a tilt surface; I_{diff} is the diffuse radiation; W is the aperture diameter of the collector; L is the length of the collector and R_b is the ratio of the beam radiation on a tilted surface to that on the horizontal surface and can be computed by equation 5.

$$R_b = \frac{\cos(\phi - \rho_t) \cos \delta_t \cos h_t + \sin(\phi - \rho_t) \sin \delta_t}{\cos \phi \cos \delta_t \cos h_t + \sin \phi \sin \delta_t} \quad \text{Eqn. 5}$$

The total heat losses in the system (Q_{losses}) is considered as the sum of the radiative heat-loss from the surface of the enveloping glass-cover to the surroundings (q_{r2}), the convective heat loss from the surface of the enveloping glass-cover to the surroundings (q_c), the radiative heat-loss from the surface of the absorber-tube to the surroundings (q_{r1}) and the conductive/convective heat loss from the fluid to the surroundings (q_1). This can be expressed as follows;

$$Q_{losses} = q_{r2} + q_c + q_{r1} + q_1 \quad \text{Eqn. 6}$$

3.3.1 Radiative Heat Loss from the Enveloping Glass-Cover to the Surroundings (q_{r2})

The radiative heat loss from the enveloping glass-cover to the surroundings (q_{r2}) is determined considering the surface area as;

$$q_{r2} = \sigma \varepsilon_g A_g (T_g^4 - T_{sky}^4) \quad \text{Eqn. 7}$$

Where σ is the Stefan-Boltzmann's constant; ε_g Emissance of the enveloping glass-cover material; A_g the surface area of the enveloping glass-cover; T_g Temperature of the enveloping glass-cover and T_{sky} the temperature of the sky given by the relation [7].

$$T_{sky} \approx T_{sur} - 6 \quad \text{Eqn. 8}$$

with T_{sur} = Ambient temperature

3.3.2 Convective Heat Loss from the Enveloping Glass-Cover to the Surroundings (q_c)

For the determination of the convective heat loss from the enveloping glass-cover to the surroundings (q_c), the Newton's law of cooling applies. Thus,

$$q_c = A_g h_c (T_g - T_{sur}) \quad \text{Eqn. 9}$$

Where h_c is the convection heat transfer coefficient of the surrounding air. This coefficient may be correlated as [8].

$$h_c = 3.8V_{wind} + 5.7 \quad \text{Eqn. 10}$$

Where V_{wind} is wind velocity and T_{sur} ambient temperature.

3.3.3 Radiative heat transfer from the absorber tube to the glass-cover (q_{r1})

The radiative energy transfer from the absorber-tube to the enveloping glass-cover (q_{r1}) is considered as radiant heat energy transfer between two gray surfaces and is given by:

$$q_{r1} = \frac{A_t \sigma (T_t^4 - T_g^4)}{\frac{1}{\varepsilon_t} + \frac{A_t}{A_g} \left[\frac{1}{\varepsilon_g} - 1 \right]} \quad \text{Eqn. 11}$$

Where A_t the surface area of the absorber tube; T_t the temperature of the absorber-tube and ε_t the emissance of the coating material on the absorber-tube.

3.3.4 Conductive/convective heat loss from the fluid to the surroundings (q_1)

The amount of heat lost by the working fluid is given as;

$$q_1 = \frac{2A_c (T_f - T_{surr})}{\frac{1}{h_c} + \frac{1}{h_f}} \quad \text{Eqn. 35}$$

Where A_c the area of the collector, h_f the convective heat transfer coefficient of the fluid, T_f the temperature of the fluid inside the tube, h_c the convection heat transfer coefficient of the surrounding air.

IV. RESULTS AND DISCUSSIONS

4.1 Results

The experiment was carried out between 08:00 to 19:00 hours daily for four months (February, March, April and May). These months are characterized by very high sunshine radiations in Bauchi and its environs, free of cloud or harmattan dust. On the contrary, June to January are characterized by cloud and rain and sometime heavy amount of harmattan dust in the air which can severely limit visibility and block the sun radiations from reaching the collector surface for several days. The readings taken were the hourly temperature of the enveloping glass-cover, absorber-tube and working fluid and the hourly topocentric angles.

4.1.1 Receiver Temperatures

Table 1 presents the monthly average experimental temperatures of glass-cover, absorber-tube, working fluid and the thermal efficiencies of the SPTC obtained hourly during the experiment. The maximum monthly average glass-cover temperature recorded was 48.3°C and the minimum was 35.1°C within the months periods investigated. The monthly average experimental temperatures of the absorber-tube increased with time and the maximum recorded was 135.6°C in the month of March, 2014. The maximum monthly average experimental temperature of the working fluid was 129.4°C recorded in April, 2014. Egbo [9] carried out the same experimental performance evaluation of the collector without considering the effects of the topocentric solar coordinates of the sun and the maximum working fluid obtained was 121.1°C. This implies that using solar position coordinates improved the performance of the collector.

4.1.2 Thermal Efficiencies

The computed monthly average experimental thermal efficiencies of the SPTC are presented in Table 1. The computation considered the dimensions, geometry and the materials of solar parabolic-trough concentrating collector (Model TE 38), thermal properties of the components of the collector are all used. The direct (E_{gd}) and reflected (E_{gr}) solar energy incident on the glass-cover and the total energy losses (Q_{losses}) in the system are equally considered for the computation of the thermal efficiencies of the SPTC.

Table 1: Average Monthly Experimental Temperatures of Glass-Cover (T_g), Absorber-Tube (T_t), Working Fluid (T_f) and Thermal Efficiencies (η_{th}) for the Months of February – May, 2014

Month	Time (hrs)	9:00	10:00	11:00	12:00	13:00	14:00	15:00	16:00	17:00	18:00	19:00
Feb.	T_g (°C)	45.0	42.8	42.9	47.4	52.1	55.3	57.3	56.1	57.8	54.7	50.4
	T_t (°C)	61.0	62.4	94.5	103.7	110.2	115.6	121.6	128.9	132.7	138.3	142.3
	T_f (°C)	48.0	62.0	87.0	110.0	120.2	122.6	123.0	124.0	120.8	122.0	122.6
	η_{th} (%)	63.9	71.7	82.3	85.1	81.8	81.9	81.0	79.6	74.2	70.5	63.5
March	T_g (°C)	45.1	45.6	47.2	49.5	52.3	53.8	53.9	54.9	55.3	52.7	50.6
	T_t (°C)	61.1	61.3	109.8	110.7	119.0	125.5	138.6	139.8	145.0	146.3	148.4
	T_f (°C)	59.0	60.3	99.3	108.9	116.5	119.0	122.8	123.5	125.6	128.8	128.6
	η_{th} (%)	61.5	73.9	78.9	78.1	77.1	75.1	72.6	70.9	70.1	60.3	50.0
April	T_g (°C)	45.0	46.6	47.8	49.5	56.0	57.0	54.0	53.2	51.0	50.2	48.5
	T_t (°C)	62.0	80.3	97.8	99.3	118.7	120.9	128.7	138.7	139.0	140.4	146.9
	T_f (°C)	57.0	66.3	87.3	98.6	110.8	119.5	127.4	129.7	130.0	132.7	132.0
	η_{th} (%)	68.0	75.0	75.4	76.1	76.0	73.8	70.0	72.4	54.5	53.7	45.3
May	T_g (°C)	45.3	43.6	43.9	49.4	52.1	56.3	58.3	55.1	57.8	55.7	51.4
	T_t (°C)	68.0	72.4	89.7	98.9	117.8	127.8	130.2	139.7	139.8	142.3	146.4
	T_f (°C)	59.0	74.5	98.5	108.7	112.5	120.8	121.5	122.9	127.3	119.4	120.1
	η_{th} (%)	71.9	76.3	80.1	85.3	84.8	85.9	79.4	74.8	73.2	60.5	48.5

4.1.3 Topocentric Incidence and Tracking angles

Table 2 presents the monthly average topocentric incidence and tracking angles in degrees respectively. As earlier discussed, the maximum amount of solar radiation reaching the reflecting surface of the collector is determined by these two angles; as they are used in aligning the axes of the collector aperture perpendicular to the sun’s central ray [6]. Thus, maximum solar radiation would be received by the collector thereby improving the performance of the collector thermal efficiency. From the Table however, the maximum incidence and tracking angles recorded experimentally were 90° and 48.8° respectively.

Table 2: Average Monthly Experimental Incidence (θ_i) and Tracking (ρ_t) Angles in Degree Recorded Hourly for the months of February-May, 2014

Month	Time (hrs)	9:00	10:00	11:00	12:00	13:00	14:00	15:00	16:00	17:00	18:00	19:00
Feb.	$\theta_i(^{\circ})$	38.0	42.9	55.0	79.5	89.9	73.5	68.9	56.3	45.8	42.5	42.9
	$\rho_t(^{\circ})$	29.5	30.1	30.8	31.4	32.0	32.6	33.2	33.7	34.2	34.8	35.3
Mar	$\theta_i(^{\circ})$	36.3	47.0	59.6	80.3	89.0	81.6	73.3	56.7	53.6	41.2	39.8
	$\rho_t(^{\circ})$	42.5	42.7	42.8	43.0	43.1	43.3	43.4	43.5	43.6	43.7	43.9
April	$\theta_i(^{\circ})$	38.8	45.6	59.9	86.4	89.8	80.6	77.9	68.1	53.4	45.6	38.9
	$\rho_t(^{\circ})$	44.9	45.0	45.3	45.7	46.1	46.6	46.9	47.3	47.5	47.9	48.3
May	$\theta_i(^{\circ})$	37.7	44.5	57.8	87.5	90.0	86.6	76.8	67.1	54.3	47.4	38.8
	$\rho_t(^{\circ})$	45.1	45.4	45.9	46.3	46.8	47.0	47.8	48.0	48.4	48.3	48.8

4.2 Discussions

4.2.1 Discussions on Experimental glass-cover Temperature

Figures 4 and 5 are the hourly average experimental temperatures of glass-cover and incidence angles plotted against time and experimental temperatures of the glass-cover and tracking angles against time for the months of February-March, 2014. The hourly temperatures of the glass-cover increased with increase in both incidence and tracking angles with time. However, during late hours of the day, the temperatures of the glass-cover decreased. This was as a result of decrease in the intensity of the solar radiation falling on the collector which reduces at sunset.

The intensity of solar radiation is largely a function of incidence angle, at which the Sun's rays strike the Earth's surface or collector aperture area. If the Sun is positioned directly overhead or 90° from the horizon, the incoming insolation strikes the surface of the Earth or the collector at right angles and is most intense. If the Sun is 45° above the horizon, the incoming insolation strikes the Earth's surface at an angle. This implies that the higher the angle of incidence the more intense the solar radiation on the collector surface [10]. The incidence angle increased as time increases during early hours of the day, thus, increasing the amount of beam radiation falling on to the collector surface and after noon hours the incidence angle decreases thus decreasing the amount of radiation falling on the collector. This implies that at a higher incidence angles the orientation of the collector focal axis to the sun central ray would be more precise, as such more direct solar radiation would be received at the receiver assembly. That was why the temperatures of the glass-cover appeared to be higher at noon hours.

The temperatures of the glass-cover are functions of tracking angles; increased in tracking angles increases the temperatures of the glass-cover as more focusing of the solar radiations would be achieved. The minimum incidence angle was 35.3° and at 90° the incidence angle is at maximum and thus maximum solar radiations are received. The maximum tracking angle attained was 48.8° and the minimum was 29.8° . Apart from hourly increased in tracking angles, the angles were also observed to increase monthly within the months investigated. This was due to seasonal variations in solar positions as the sun central ray moves between the two tropics (i.e. tropic of Cancer and tropic of Capricorn).

The transmissivity of the glass-cover and energy losses from the glass-cover to surroundings may result in making the temperatures of the glass-cover to be low, the higher the transmissivity of the material the more the solar radiation being transmitted to the absorber-tube, thus less temperature at the glass-cover surface would be experienced. This may increase the performance of the SPTC as more temperature is being received by the absorber-tube.

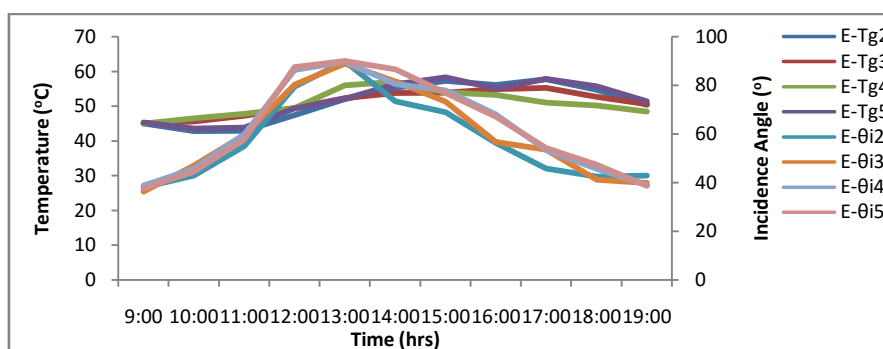


Fig.4: Experimental Glass-cover Temperatures and Incidence angles against Time

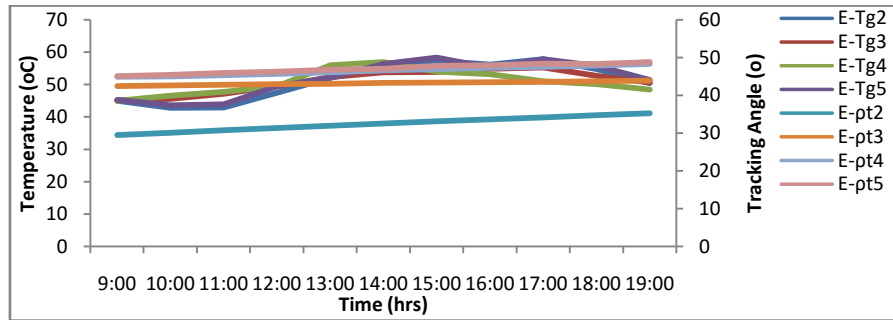


Fig.5: Experimental Glass-cover Temperatures and Tracking Angles against Time

4.2.2 Discussions on Experimental Absorber-tube Temperature

Figure 6 and 7 presents the monthly averages of absorber-tube temperatures, incidence and tracking angles plotted against time for the four month period investigated. They both show remarkable increased in temperatures with time. The progressive increased in temperatures of the absorber-tube was as a result of high transmissivity of the glass-cover which permits direct solar radiation to pass through it, the absorber-tube which is being painted black (high absorptivity rate and low emittance) and the annular gap of the receiver being evacuated; thus, reduced the convective heat losses between the glass-cover and the absorber-tube thereby making the tube temperature to be building up progressively. The maximum temperature recorded was 148.4°C in March and the minimum was 61.0°C February, 2014. The effects of the incidence and tracking angles on the absorber-tube temperatures are as explained in section 4.2.1. They both increased the rate of heat absorption by the absorber-tube as more solar energy would be focus onto the receiver assembly.

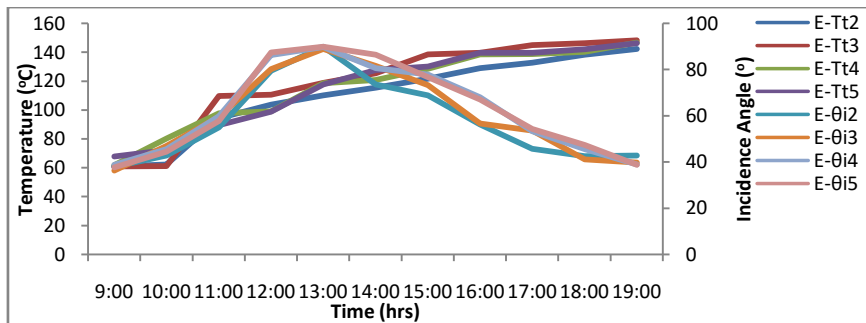


Fig.6: Experimental Absorber-tube Temperatures and Incidence Angles against Time

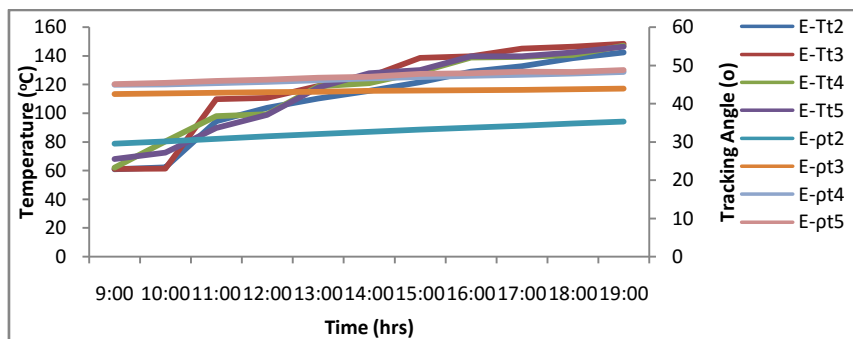


Fig.7: Experimental Absorber-tube Temperatures and Tracking Angles against Time

4.2.3 Discussions on Experimental Working Fluid Temperature

The monthly average of experimental temperatures of the working fluid increased with time as shown in Figures 8 and 9. The effects of the incidence and tracking angles are as discussed in section 4.2.1. The incidence angle increased with time in the early hours to a maximum at noon and gradually decreases until sunset. The tracking angles as well increased to a maximum at 19:00hrs.

The increased in temperatures of the working fluid were achieved as a result of conductive and convective heat transfers from the absorber-tube to the fluid which increased with time, thereby transferring more heat energy to the fluid. When the temperature difference between the fluid and the contact surface causes density variation in the fluid, convective heat transfer takes place and thus heat is being transferred from the

tube to the fluid. The rate at which heat is actively removed from the absorber-tube to the fluid determines the operating temperature of the collector. The copper tube used as the absorber-tube was coated with emulsion black paint that has low emittance and thus, enhances the absorption of the incident solar irradiance and reduction in the reflectance, thus increases the amount of heat transferred to the fluid. Also, the annular gap of the receiver being evacuated aids in suppressing the convective heat losses between the glass-cover and the absorber-tube.

The maximum temperature of working fluid recorded by Egbo[9] was 121.1°C and this is less than the maximum working fluid temperature recorded during this work (132.7°C). This means that the used of solar coordinates in tracking the sun has better solar radiation collection, thus the increased in the thermal performance of the collector. The temperatures obtained experimentally are capable to boil water and other coolant that has low boiling point; consequently, steam can be generated for electricity generation and other applications.

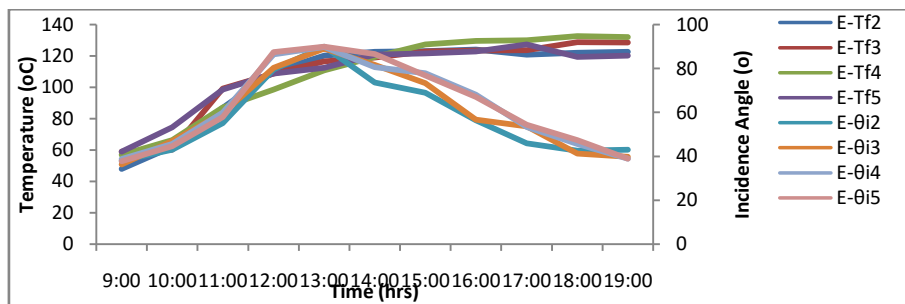


Fig.8: Experimental Working Fluid Temperatures and Incidence Angles against Time

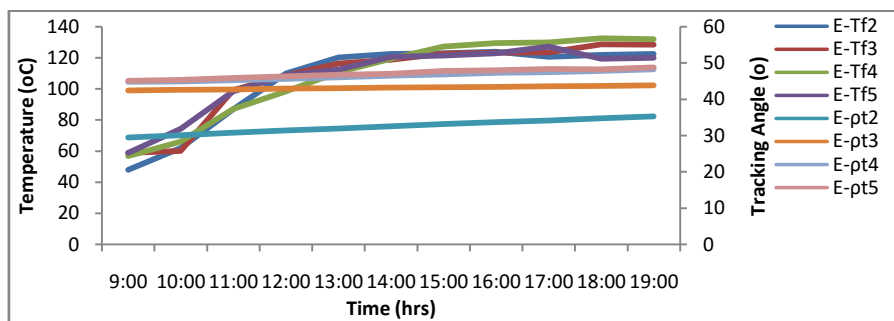


Fig.9: Experimental Working Fluid Temperatures and Tracking Angles against Time

5.2.3 Discussions on Experimental Thermal Efficiencies of the SPTC

The monthly average experimental thermal efficiencies of the SPTC and incidence angles are plotted against time as shown in Figure 10. Figure 11 however, was the thermal efficiencies and tracking angles against time for February, March, April and May investigated. From these two Figures, it was observed that the thermal efficiencies of the SPTC increased as the time increases. This was as a result of increased in both the incidence and tracking angles as time increases. When there is an increased in both the incidence and tracking angles more focusing of the sun central ray would be achieved, thus more direct solar radiations would be received onto the receiver assembly. However, after noon hours the incidence angles decreased which lead to the decreased in solar radiations falling on the collector due to cosine effects. Consequently, decreases the thermal efficiencies of the SPTC.

Increased solar radiation results in increased solar energy absorbed by the collector. It should be noted that thermal losses also increase due to the increased collector temperature. However, this increase in thermal losses is smaller than the enhanced absorbed solar energy. Adel *et al*[11] carried out an investigation on the performance analysis of parabolic trough collector in hot climate and discovered that the efficiency of a SPTC increased when angle of incidence increases. This is in agreement with this work as the incidence angles increases, the collector thermal efficiencies increased. The early increase in thermal efficiency observed in this work was as a result of temperature building up in the system. As sunsets, the intensity of the solar radiation reduces; consequently reduces the rate of heat being collected by the collector and transmitted to the receiver assembly and thus reduced the thermal performance of the SPTC.

The behaviors of the collector thermal efficiencies and tracking angle against time exhibited by these graphs are in consonant with that of the thermal efficiencies and incidence angles against time. As the tracking angles increases with an increase in time, the thermal performance of the collector also increases. More focusing

of the solar beam radiation on to the collector aperture area was achieved as the tracking angle increased. Thus, the collector tends to collect more solar radiation with increased in the tracking angle thereby increasing the performance of the collector. However, it was observed that the degree of increase in tracking angle is relatively small; this is due to the collector orientation that was placed in east-west direction which require little tracking. According to Kalogirou [12], the trough can be oriented either in an east-west direction, tracking the sun from north to south, or orientated in a north-south direction and tracking the sun from east to west. The advantages of the former tracking mode is that very little collector adjustment is required during the day and the full aperture always faces the sun at noon time but the collector performance during the early and late hours of the day is greatly reduced. This is evidently vindicated by this work, as the early and late hours of the thermal performance of the collector are low.

Over the period of one year, a horizontal north-south collector trough field usually collects slightly more energy than a horizontal east-west one. However, the north-south field collects a lot of energy in summer and much less in winter. The east-west field collects more energy in the winter than a north-south field and less in summer, providing a more constant annual output and this serve as an added advantage [12]. These arguments were also corroborated by Zarza *et al*[13]. According to Zarza *et al*[13], the thermal energy produced by a solar field with SPTC whose axis is North-South oriented varies a lot during the year. Three to four times more energy is delivered daily during summer months than in winter months. Thermal energy delivered by SPTC with axis oriented east-west does not vary as much from summer to winter. This is another added advantage enjoyed by this work as the collector was oriented in east-west axis.

Arasu and Sornakumar[14], Egbo[9] and Milton *et al*[15] both conducted a research on performance evaluation of parabolic trough solar collector system and discovered that both the predicted and observed thermal efficiencies of solar parabolic trough collector range between 88.3% - 69.1%. The works of Brooks *et al*[16] for both evacuated glass shielded receiver and unshielded receiver were between 53.8%-55.2% peak thermal efficiencies. The maximum experimental thermal efficiency obtained in this work was 85.9% in May and the minimum was 45.3% April, 2014.

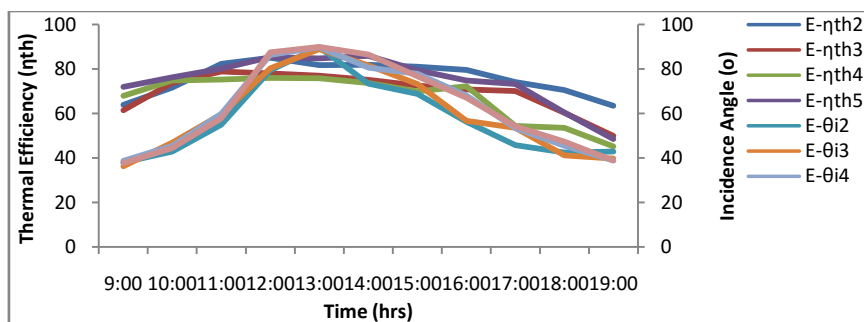


Fig.10: Experimental Thermal Efficiencies and Incidence Angles against Time

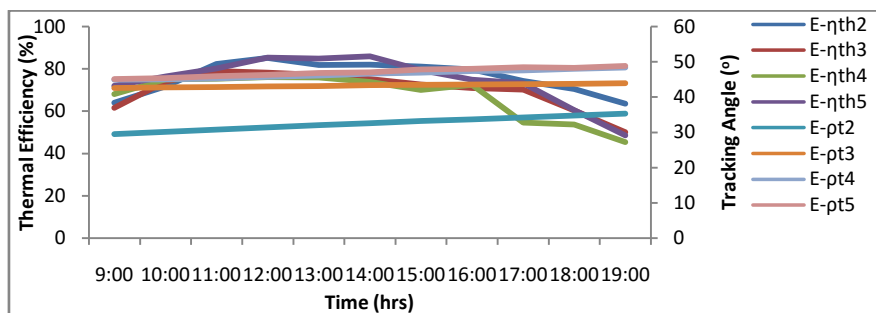


Fig.11: Experimental Thermal Efficiencies and Tracking Angles against Time

V. CONCLUSION

Experimental performance evaluation of solar parabolic-trough collector using solar position coordinates of Bauchi was carried out and from the results obtained, the hourly temperatures of the glass-cover, absorber-tube and the working fluid increased with increased in both incidence and tracking angles with time. The maximum temperatures of glass-cover, absorber-tube and working fluid attained are 58.3°C, 148.4°C and 132.7°C respectively. The absorber-tube temperatures attained experimentally are capable of boiling water and other low boiling point coolant for steam generation and thus for generating electricity and other solar water applications. The effects of using solar coordinates influence the performance of the collector. The thermal

efficiency of the collector increased as the incidence and tracking angle increases with time and the maximum attained was 85.9%. The system can be scale up for energy generation and integration into the national energy mix of Nigeria.

REFERENCES

- [1]. Jesuleye, O. A. and Siyanbola, W. O. (2008), Solar Electrification Demand Analysis for Improved Access to Energy Services in Nigeria. *Nigerian Journal of Solar Energy*. 19:1
- [2]. Sintali, I. S. Egbo, G. and Dandakouta, H. (2014). Energy Equations for the Computation of Parabolic-Trough Collector Efficiency Using Solar Positions Coordinates. *American Journal of Engineering Research*. 3(10):25-33
- [3]. Plint and Partners LTD Engineering (1984); Laboratory Manual; England pp2-26
- [4]. Harrison, J. (2001). Investigation of Polycarbonate as a suitable "Greenhouse" material for Solar Cooker. Florida Solar Energy Centre, USA.
- [5]. Nigerian Meteorological Agency (NIMET). (20013). Bauchi Airport, Bauchi.
- [6]. Williams, B. and Geyer, M. (2003). Power from the Sun. Retrieved March 03, 2004; from: <http://www.powerfromthesun.net/book>
- [7]. Duffie, J. A. and Williams, A. B. [Ed.] (2006): *Solar Energy Thermal Processes*. John-Wiley and Sons, New York
- [8]. Sukhatme, S. P. (1991). *Solar Energy: Principles of Thermal collection and Storage*. Tata McGraw-hill Publishing Company Limited. India
- [9]. Egbo, G. (2008). Experimental Performance Evaluation of a Solar Parabolic-Trough Collector Model (TE38) in Bauchi. *International Journal of Pure and Applied Sciences*. 2(1):55-64.
- [10]. Anonymous: "Energy and Matter" Earth-Sun Relationship, Retrieved from <http://www.physicalgeography.net/fundamentals/htmlon14/11/15>
- [11]. Adel, A. G.; Adel, M. M.; and Kandil, M. K. (2014). Performance Analysis of Parabolic Trough Collector in Hot Climate. *British Journal of Applied Science & Technology*, 4(14): 2038-2058.
- [12]. Kalogirou, S. A. (2004). *Solar Thermal Collectors and Applications*; Progress in Energy and Combustion Science, Elsevier 30:231-295
- [13]. Zarza E.; Valenzuela L. and Leon J. (2012). Solar Thermal Power Plants with Parabolic-Trough Collector. Proceeding of 2nd Plataforma Solar de Almeria-CIEMAT, Apdo 22, E-04200, Almeria, Spain.
- [14]. Arasu, A. V. and Sornakumar, T. (2006). Performance Characteristics of Solar Parabolic trough Collector System for Hot water Generation. *International Energy Journal*. 7(2):137-144
- [15]. Milton, M. R., Naum, F. and Chiguero, T. (2009). Analytic Modeling of a Solar Plant with Parabolic Linear Collectors. Elsevier, *Solar Energy*. 83:126-133
- [16]. Brooks, M. J., Mills, I. and Harms, T. M. (2006). Performance of a Parabolic Trough Solar Collector. *Journal of Energy in Southern Africa*. 17:71-80.